SAND2016-2072C

2016 Spring Meeting of the Western States Section of the Combustion Institute
hosted by the University of Washington
March 21-22, 2016

Quantifying Soot Concentrations in Turbulent Non-Premixed Jet Flames

Christopher R. Shaddix, Jiayao Zhang, and Timothy C. Williams

Combustion Research Facility
Sandia National Laboratories
Livermore, CA 94550 USA

Truly quantifying soot concentrations within turbulent flames is a difficult prospect. Laser extinction measurements are constrained by spatial resolution limitations and by uncertainty in the local soot extinction coefficient. Laser-induced incandescence (LII) measurements rely on calibration against extinction and thereby are plagued by uncertainty in the extinction coefficient. In addition, the LII measurements are subject to signal trapping in flames with significant soot concentrations and/or flame widths. In the study reported here, a turbulent ethylene non-premixed jet flame (jet exit Reynolds number of 20,000) is investigated by a combination of LII and full-flame HeNe laser (633 nm) extinction measurements. The LII measurements have been calibrated against extinction measurements in a laminar ethylene flame. An extinction coefficient previously measured in laminar ethylene flames is used as the basis of the calibration. The time-averaged LII data in the turbulent flame has been corrected for signal trapping, which is shown to be significant in this flame, and then the line-of-sight extinction for a theoretical 633 nm light source has been calculated across the LII-determined soot concentration field. Comparison of the LII-based extinction with that actual measured along the flame centerline is favorable, showing an average deviation of approximately 10%. This lends credence to the measured values of soot concentrations in the flame and also gives a good indication of the level of uncertainty in the measured soot concentrations, subject to the additional uncertainty in the previously measured extinction coefficient, estimated to be ±15%.

1. Introduction

The health effects of fine particulate matter (PM) in ambient air have become increasingly evident over the past decade. These particles are able to deeply penetrate lung tissue and have been shown to have a number of deleterious effects associated with the pulmonary and cardiovascular systems, leading to increased morbidity and mortality [1-6]. Because of this association between fine PM in the atmosphere and deleterious health, soot emissions from internal combustion engines and aviation gas turbine engines have faced increasingly stringent regulation. In addition, national and regional regulatory agencies have been decreasing the maximum fine PM permitted in the atmosphere according to ambient air quality standards and in this regard have shown concern over aircraft emissions associated with airports and military bases. Furthermore, in-flight emission of fine particulates from gas turbine engines has been shown to have effects on contrail/cloud formation and climate forcing [7,8].

In light of these concerns, there is a strong desire among aircraft engine designers to have a truly predictive modeling capability for soot formation and emission, considering the influence of changes in the fuel composition, ambient conditions, and engine design and operation. At this moment, such a capability is still lacking. One reason for the lack of predictive models of soot formation in the complex gas turbine combustion environment is the lack of robust, spatially and temporally resolved data in turbulent reacting flow fields, specifically for sooting fuels. Such datasets have been in development for many years for soot-free flames [9] and more recently for a slightly sooting methane flame [10], but available experimental datasets for moderate sooting turbulent flames are largely lacking. Such datasets are needed because under moderately sooting flame conditions, believed to be representative of aviation gas turbine combustors, the soot that is formed radiates energy away from the hottest soot-containing regions to the walls and to the cooler soot-containing regions, thus redistributing the reaction enthalpy and influencing the flame chemistry and burning rate in a

coupled manner [11]. The ability of computational models to accurately describe these coupled soot formation/radiation/flame chemistry interactions cannot be tested with data from soot-free or lightly sooting flames.

Previously, we have reported on the design of piloted, turbulent jet flame burners for using higher hydrocarbon fuels, specifically on two designs for studying ethylene flames and for studying flames fueled by prevaporized aviation fuel [12]. Nominal results for soot laser-induced incandescence (LII) and OH planar laser-induced fluorescence (PLIF) have been previously reported in canonical ethylene and JP-8 surrogate jet flames with a fuel exit Reynolds number of 20,000 [13]. In addition, preliminary results for the joint soot temperature-volume fraction statistics, as determined with a '3-line' laser-optical diagnostic approach, were also previously reported for these flames [14].

In this paper we describe how the LII measured soot volume fraction can be corrected for signal trapping, at least on a time-averaged basis, and then use the trapping-corrected LII measurements to calculate the time-averaged extinction of a HeNe laser (633 nm) across the flame. The computed centerline profile of laser extinction as a function of axial position is then compared against the measured full-flame extinction, from which an assessment can be made of the quantitative accuracy of the time-averaged, trapping-corrected soot concentration field. A full assessment of the uncertainty in the determined soot concentration field must also consider uncertainty in the value of the dimensionless extinction coefficient used to interpret the extinction measurements and to calibrate the LII, which is also discussed here.

2. Methods

Measurements were performed in a piloted turbulent non-premixed ethylene jet flame stabilized on a burner designed along the same principle as the well-known Sydney burner [15] with a central fuel tube (3.2 mm ID) and a concentric outer tube (19.1 mm OD). A pilot plate is situated in the annulus between the two tubes and near the lip and contains three concentric rows of equally distributed holes, supporting tiny flames for stabilizing the primary jet flame. While the central jet was composed of pure ethylene, a premixed ethylene/air mixture at an equivalence ratio of 0.9 was supplied to the pilot holes at a flow rate corresponding to 2% of the energy release rate of the main jet. With this design, the jet flames showed good flame attachment, even for fuel jet Reynolds numbers (Re) exceeding 30,000. The burner was positioned on top of a vertical wind tunnel that provided co-flowing dry air at 0.6 m/s, to prevent room-air disturbance and provide well-established boundary conditions for flame modeling. The whole assembly was mounted on a platform with XYZ translation to easily change the flame measurement location.

A flame with a fuel jet Reynolds number of 20,000 (corresponding to a fuel mass flow rate of 26.4 slpm at 298 K) was investigated in this study. This flame has sufficiently strong turbulence to minimize the influence of buoyancy and to test the robustness of combustion models, but avoids frequent local flame extinction events in the high-shear region just above the burner lip (as verified with OH PLIF imaging [12]). The existence of flame extinction and subsequent reignition poses a major challenge for flame modeling [16], even in the absence of soot and its associated radiant heat transfer. For the broadest applicability to turbulent flame modeling in the near-term, it seemed prudent to perform measurements in a flame without significant local extinction. The heat release rate of the flame was 24.0 kW and it had a visible flame height of approximately 870 mm.

The fundamental infrared (IR) output of a Nd:YAG laser (1064 nm) was used to excite the LII. The laser operated at 10 Hz and had a nominal pulse duration of 10 ns. The use of IR excitation instead of the commonly used 532 nm excitation offers the advantages of substantially reduced photochemical interference from other species, such as C_2 or C_3 [17,18], as well as significantly reduced laser extinction across the flame. Further, with IR laser excitation longer wavelength visible wavelengths could be used to capture the LII signal, reducing its sensitivity to signal trapping. The laser beam was expanded through a concave cylindrical lens (focal length = –75 mm) and shaped into a vertically collimated laser sheet by passing through a convex spherical lens (focal length = 1000 mm). An iris placed between the lenses and the burner trimmed the laser sheet to a height of 47 mm. The thickness of the laser sheet, defined as the $1/e^2$ width, was found to be 275 μm, respectively, with a variation of less than 15% across the field-of-view of the imaging camera. A laser pulse energy of 66 mJ was used, giving a fluence of 0.6 J/cm^2. A measurement of the LII fluence response (Fig. 1) found a nominal laser fluence 'plateau region' from 0.3 to 0.7 J/cm^2, in which the LII signal was relatively insensitive to the change in laser fluence. Therefore, the LII signal was nearly independent of minor shot-to-shot fluctuations in the laser power or attenuation of the laser sheet (up to 50%) as it passed through the sooty flame.

The LII signals were collected by a Princeton Instruments intensified, fast-gating CCD (ICCD) camera mounted perpendicular to the laser path. The camera had a full-frame 512×512 CCD array and was set to image an area of 60×60 mm^2 (117 μm on each pixel). It was equipped with a Nikkor 50-mm focal length f/1.2 lens (Nikon), whose aperture was stepped down to f/2 in order to minimize optical aberrations (primarily coma) in the peripheral region of the field-of-view. LII signal was collected through a Schott BG-14 glass filter and a 600-nm short-pass filter, effectively accepting

light from 300 to 600 nm. This detection band encompasses the peak spectral range of soot incandescence [17,19] while rejecting natural soot luminosity in the red and near-IR. The camera gate was set to 50 ns with zero delay from the IR laser pulse. This prompt-detection scheme lessens the bias towards large soot particles that is evident for detection with a longer gate and/or a delayed gate opening [17,19].

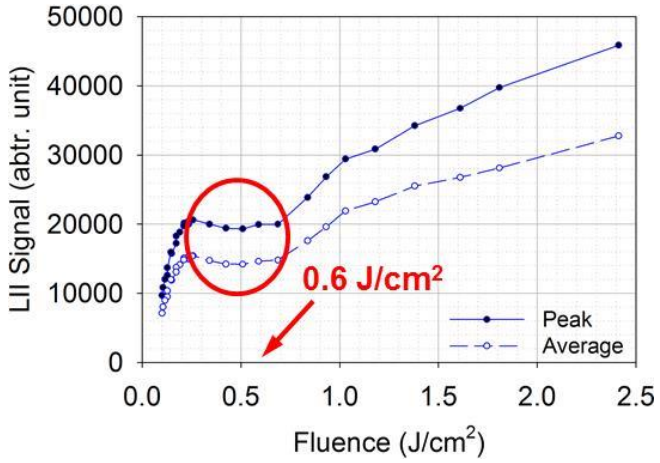

Figure 1. Dependence of soot LII signal on the incident laser fluence for the experimental configuration used here, measured within a laminar ethylene flame at 35 mm above the burner exit. Solid and dashed lines represent peak and spatially averaged values of the soot-containing region of the flame cross-section. The laser fluence was varied using a half-wave plate to rotate the polarization of the laser beam before passing it through a glan-laser polarizer. The circle highlights the 'plateau region' and the arrow denotes the fluence level used for the LII measurements of soot concentration.

The LII signals were calibrated for soot volume fraction by performing both LII imaging and laser extinction measurements with a cw HeNe laser (632.8 nm) on a laminar ethylene jet flame with a cold flow velocity of 0.41 m/s, anchored on the same jet burner as used for the turbulent flame. This flame had a flame height of about 70 mm and a peak soot concentration of 4.1 ppm. For the extinction measurement, a continuous reference laser intensity measurement was captured on a photodiode from the reflection off of an angled optical flat. The transmitted laser light was collected in an integrating sphere and then detected on a photodiode after passing through a laser line filter. For measurements in laminar flames the use of the integrating sphere is unnecessary to collect all of the transmitted light. However, the same extinction measurement was also performed across the turbulent flame, where transient beam steering of the bam through the flame makes use of the integrating sphere necessary.

Quantification of the measured extinction in terms of soot volume fraction requires application of the Beer-Lambert-Bouguer Law for absorption and scattering from small particles [20]:

$$I/I_0 = e^{-KL} = e^{\frac{-K_e f_v}{\lambda} L}$$

where KL is the optical depth of the interrogated field, K_e is the dimensionless extinction coefficient, f_v is the soot volume fraction, λ is the wavelength of light, and L is the optical pathlength containing soot. Soot particles primarily absorb light, particularly when unagglomerated, because of their small size and their relatively strong absorptivity over a broad range of wavelengths. For this reason, many researchers have ignored soot scattering contributions to the extinction coefficient and have deduced soot volume fraction from extinction measurements using Rayleigh-limit soot absorptivity coefficients calculated from literature values of soot index of refraction. This poses a problem because there is a wide range of soot index of refraction values in the literature, leading to highly variable deduced soot volume fractions for a given extinction measurement [21]. Furthermore, more recent direct measurements of the dimensionless extinction coefficient suggest that interpretations of extinction with absorption coefficients deduced from common soot index of refraction values in the literature overestimate the soot concentrations by a factor of two to three [22, 23]. A small portion of this difference (up to approximately 30%) may be ascribed to the contributions of soot scattering to the

extinction for agglomerated soot, but the majority of the difference must be ascribed to errors in the determination of the soot index of refraction [24-26]. In fact, determination of soot refractive index traditionally has relied on collection of bulk samples of soot and compressing it into a smooth pellet, which is problematic for agglomerated nanoparticles like soot. Furthermore, the bulk soot collection has involved the use of cooled metallic probes placed into sooty regions of flames [27], wherein one can imagine soot precursor particles and even heavy PAH species will be collected into a deposit, along with truly solid, graphitic soot. Our previous investigation collecting soot even when using uncooled probes in diffusion flames showed a significant fraction of the collected soot material consisted of methylene chlorine extractable material in the active soot formation region of the flames [26].

Given the uncertainty of determining a true, characteristic index of refraction for black soot and ambiguity about the variation in the scattering albedo in different regions of a flame, a more defensible approach to quantifying the measured soot extinction is to use a dimensionless extinction coefficient (or equivalently, for a given wavelength, to use a given value of the function E(m), where E(m) is defined to be equal to $K_e/6\pi$). For this reason, we choose here to use a dimensionless extinction coefficient, K_e, of 9.3, which is an average of those determined for soot sampled from laminar ethylene diffusion flames by Williams et al. [26] and which also corresponds to a midpoint value of the range of dimensionless extinction coefficients measured from soot emitted from both laminar and turbulent flames [26]. Based on the range of reported variation in K_e measurements from numerous investigators and flames from values of 8 to 10, the 2σ uncertainty in K_e for solid, graphitic soot is estimated to be ± 15%.

3. Results and Discussion

Figure 2 shows the planar soot volume fraction LII image data for the turbulent ethylene jet flame, including instantaneous snapshots, the temporal mean, and the root mean square (rms) variations in soot concentration, expressed in terms of parts per million (ppm) by volume after calibration against the extinction measurements in the laminar ethylene flame.

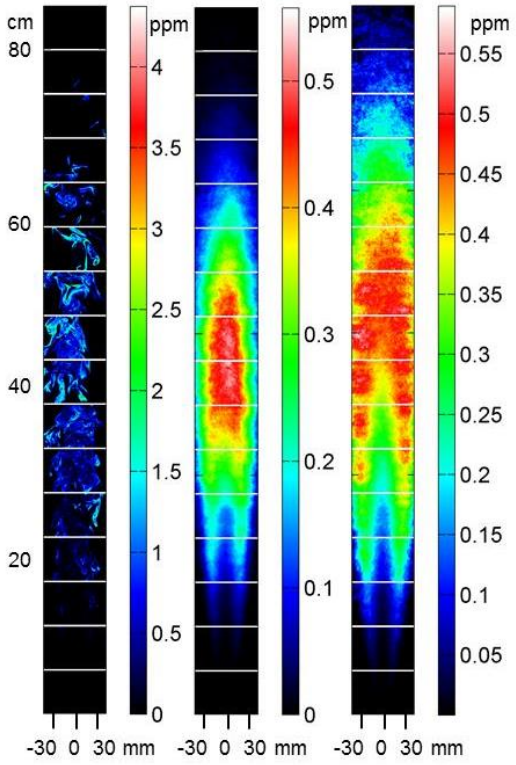

Figure 2. Instantaneous, mean, and rms (left-to-right) of soot volume fractions measured by LII imaging in the turbulent ethylene jet flame. The instantaneous image is a collage of images taken at different heights.

It is evident from Fig. 2 that the soot field is highly intermittent in this turbulent flame. The peak values of soot concentration in the instantaneous images are in the neighborhood of 4 ppm, similar to the maximum soot concentrations (when using the K_e value used here) in laminar ethylene flames, whereas the mean soot concentration peaks at 0.5 ppm. Further evidence of the strong intermittency is shown by the rms values, whose magnitudes are similar to the mean values throughout the primary sooting region of the flame. Figure 3 shows a selection of horizontal profiles of mean soot concentration through the flame. It is evident that turbulent mixing processes bring soot occasionally out to quite wide radial positions (> 60 mm from the centerline).

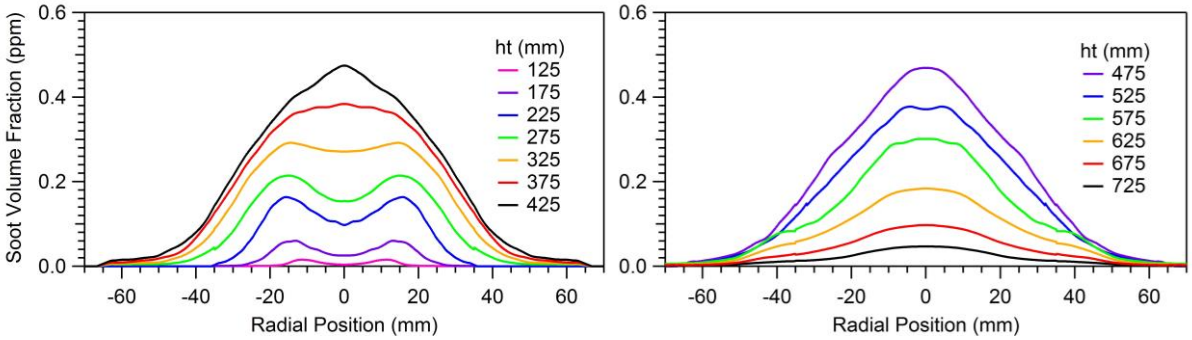

Figure 3. Symmetrized (averaged about the centerline) time-averaged soot volume fraction profiles in the ethylene jet flame, at 50 mm intervals of height.

The measured mean extinction of 633 nm laser light across the flame peaks at 33%, which indicates a mean signal trapping of the LII signal on the order of ½ of this amount (because the LII signal only needs to propagate half-way through the flame). To correct the time-averaged LII signals for signal trapping, we employ an onion-peeling routine previously described by Shaddix et al. [28]. Recent numerical analysis has shown that because of the three-dimensional nature of LII signal propagation and the pronounced forward-scattering nature of soot, scattering losses from LII signal propagation out of a sooty flame are offset by scattering gain from LII signal that was originally not directed towards the detector, such that a dimensionless *absorption* coefficient, rather than an *extinction* coefficient, should be used to compute the signal trapping loss when exciting LII with a laser sheet [29]. Therefore, we employ here an assumed K_a = 7.4 for visible LII signals, as deduced by Bond and Bergstrom [30] in a review of the optical properties of black carbon in the atmosphere (i.e. from emitted soot particles). This value for K_a is further bolstered by the measurements of Williams et al. [26] for weakly agglomerated methane soot particles, for which K_a was determined to be between 7 and 8. Also, a K_a value of 7.4, combined with a K_e value of 9.3, denotes an assumption of a scattering albedo of 20%, which is appropriate for moderately agglomerated soot particles as expected in this type of flame [31,32].

With this selection of K_a, the signal trapping corrections are shown in Fig. 4. Because the mean soot profiles do not generally show a substantial annular character, except near the bottom of the flame, the signal trapping effect is generally greatest at the flame centerline (in contrast to the trapping effect in typical laminar diffusion flames, which exhibit a strong annular soot characteristic [28]). It is evident that neglecting the signal trapping correction would lead to an error of 16% for the maximum mean soot volume fraction in this flame. Further, LII signal collection at shorter wavelengths than used here (with a 600 nm short pass filter), as is often done, will lead to correspondingly larger signal trapping effects, due to the nominally 1/lambda dependence of soot particle absorption at visible wavelengths [23].

Fig. 5 gives the trapping-corrected time-averaged LII soot concentrations, which peak at just under 0.6 ppm. These concentrations compare favorably to those that have been reported for other turbulent ethylene jet flames, once corrections are made for the assumed dimensionless extinction coefficient used to quantify the soot concentrations. For example, Coppalle and Joyeaux [33] studied an ethylene jet flame with Re = 11800, supported on a tube of 4 mm diameter and measured a peak time-averaged soot volume fraction of 1.9 ppm, at a height of 380 mm, when using a probe-based laser extinction technique and an assumed K_e of 3.5. Their peak concentration corresponds to 0.7 ppm when using a K_e of 9.3, as supported by recent measurements and as used in the current study. Hu et al. [31] investigated an ethylene flame with Re = 13500 on a 4.5 mm tube diameter and found the peak mean soot volume fraction to be approximately 1.2 ppm, when using probe-based laser extinction and an assumed K_e of 3.7. This corresponds to a value

of 0.5 in the context of the current study. Lee et al. [34] investigated ethylene jet flames with Re varying from 4000 to 23000. They found a peak mean soot volume fraction of approximately 1 ppm for flames with Re near 20000, when using an assumed K_e of 4.9 to calibrate their LII measurements. In the context of the current study, the peak mean soot volume fraction corresponds to 0.5 ppm, which is very consistent with the results here, considering that Lee et al. did not employ a signal trapping correction to their LII detection at 400 nm. Lee et al. also found the soot concentration rms to be of similar magnitude to the mean concentration, consistent with the results here.

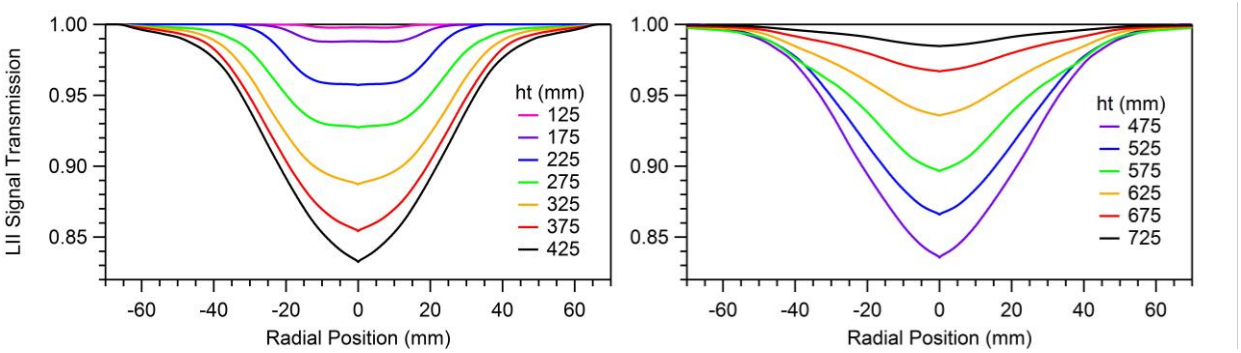

Figure 4. Calculated LII signal trapping for the soot concentration profiles shown in Fig. 3.

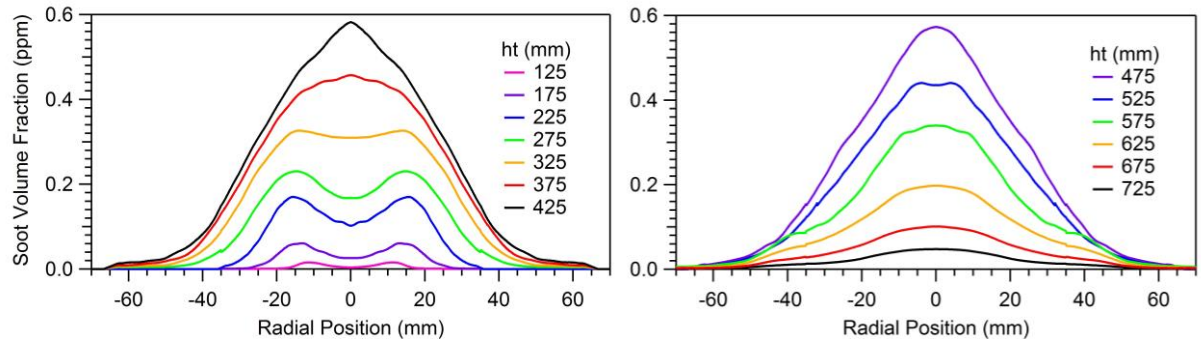

Figure 5. Signal-trapping corrected, time-averaged soot volume fraction profiles in the ethylene jet flame.

A final, semi-independent check of the accuracy of the LII data calibration and signal trapping procedure can be made by comparing the full-flame laser extinction measurements against the extinction amount that the corrected LII measurements would predict, using the same K_e value as assumed in interpreting the LII calibration in the laminar flame. This comparison is shown as a function of height in the turbulent jet flame in Fig. 6. As is apparent, the agreement between the predicted laser extinction and the actual measured laser extinction is remarkably good, with the LII matching the measured extinction nearly perfectly over the lower half of the flame and overestimating the measured extinction by 10-20% over the upper portion of the flame. This overestimation of the integrated soot in the higher portions of the flame may be due to the thickening of the LII laser sheet at greater radial distances in combination with a strong laser intensity on the far side of the laser fluence signal plateau region, leading to overestimation of soot concentrations far away from the flame centerline. As the flame spreads radially with height, the probability of soot existing at significant radial positions increases with height. Still, the overall agreement in Fig. 6 is remarkable.

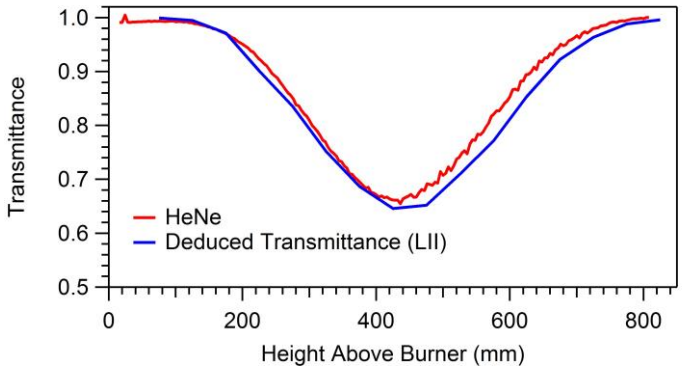

Figure 6. Comparison of measured centerline transmittance of a HeNe laser beam across the turbulent ethylene jet flame and the 633 nm transmittance deduced from the LII-determined soot volume fraction field, after correction for signal trapping.

4. Conclusions

True quantification of soot concentration measurements in turbulent flames is difficult, particularly in consideration of the effect of signal trapping on the measured optical signals. On a time-averaged basis, a signal trapping correction can be employed, to the extent that the absorption coefficient of the soot is well known. Similarly, quantification of the extinction and LII measurements requires good knowledge of the soot extinction coefficient. In the study reported here, extinction-calibrated LII measurements were used to quantify soot concentrations in a moderately turbulent piloted non-premixed ethylene jet flame. The best-available information was used to calibrate the LII measurements and to apply a signal trapping correction. Once this had been done, the corrected LII measurements were used to calculate the extinction of a 633 nm laser beam across the flame as a function of height, and this was compared against actual HeNe laser extinction measurements across the flame. The comparison was quite favorable, giving an average deviation in the deduced extinction of about 10%. This comparison, together with an estimated uncertainty of the soot absorption and extinction coefficients of ±15%, gives a defensible confidence in the quantification of the soot concentrations in these types of flames.

Acknowledgements

This work was supported by the U.S. DoD's Strategic Environmental Research and Development Program (SERDP). Sandia is a multi-program laboratory operated by Sandia Corporation, a Lockheed Martin Company, for DOE's National Nuclear Security Administration under Contract DE-AC04-94AL85000.

References

[1] F. Laden, L.M. Neas, D.W. Dockery, J. Schwartz, *Envir. Health Persp.* 108 (2000) 941-947.
[2] C.A. Pope, R.T. Burnett, M.J. Thun, E.E. Calle, D. Krewski, K. Ito, G.D. Thurston, *JAMA* 287 (2002) 1132-1141.
[3] C. de Haar, I. Hassing, M. Bol, R. Bleumink, R. Pieters, *Toxic. Sciences* 87 (2005) 409-418.
[4] R.B. Schlesinger, N. Kunzli, G.M. Hidy, T. Gotschi, M. Jerrett, *Inhalation Toxic.* 18 (2006) 95-125.
[5] M.R. Heal, P. Kumar, R.M. Harrison, *Chem. Soc. Rev.* 41 (2012) 6606–6630.
[6] A.C. Rohr, R.E. Wyzga, *Atmos. Envir.* 62 (2012) 130-152.
[7] R. Watson, J. Houghton, D. Yihui, B. Metz, O. Davidson, N. Sundararaman, D. Griggs, D. Dokken, *Aviation and the Global Atmosphere*, a special report of the Intergovernmental Panel on Climate Change (IPCC), 1999, available from http://www.ipcc.ch/ipccreports/sres/aviation/index.htm .
[8] T.C. Bond, S.J. Doherty, D.W. Fahey, et al. J. Geophys. Res. Atm. doi: 10.1002/jgrd.50171.
[9] R.S. Barlow, *Proc. Combust. Instit.* 31 (2007) 49-75.
[10] N.H. Qamar, Z.T. Alwahabi, Q.N. Chan, G.J. Nathan, D. Roekaerts, K.D. King, *Combust. Flame* 156 (2009) 1339-1347.
[11] A. Gupta, D.C. Haworth, M.F. Modest, *Proc. Combust. Instit.* 34 (2013) 1281-1288.
[12] J. Zhang, C.R. Shaddix, R.W. Schefer, *Rev. Sci. Instr.*82 (2011) 074101.

[13] J. Zhang, C.R. Shaddix, R.W. Schefer, Proceedings of the Western States Section of the Combustion Institute, Paper 09F-57, Oct. 26-27, 2009, UC Irvine, Irvine, CA.
[14] C.R. Shaddix, J. Zhang, Proceedings of the 8th US National Combustion Meeting, Paper 070LT-0100, May 19-22, 2013, Park City, UT.
[15] A.R. Masri, R.W. Dibble, R.S. Barlow *Prog. Energy Combust. Sci.* 22 (1996) 307-362.
[16] K. Gkagkas, R.P. Lindstedt, T.S. Kuan, *Flow Turb. Combust.* 82 (2009) 493-509.
[17] R.L. Vander Wal, *Appl. Optics* 35 (1996) 6548-6548.
[18] F. Goulay, P.E. Schrader, L. Nemes, M.A. Dansson, H.A. Michelsen, *Proc. Combust. Instit.* 32 (2009) 963-970.
[19] R.J. Santoro, C.R. Shaddix, in: K. Kohse-Höinghaus and J. Jeffries (Eds), Applied Combustion Diagnostics (Taylor & Francis, New York), 2002, p. 252.
[20] M. Kerker, The Scattering of Light (Academic Press, New York), 1969, pp. 31-39.
[21] K.C. Smyth, C.R. Shaddix, *Combust. Flame* 107 (1996) 314-320.
[22] M.Y. Choi, G.W. Mulholland, A. Hamins, T. Kashiwagi, *Combust. Flame* 102 (1995) 161-169.
[23] S.S. Krishnan, K.C. Lin, G.M. Faeth, *J. Heat Trans.* 122 (2000) 517-524.
[24] G.W. Mulholland, R.D. Mountain, *Combust. Flame* 119 (1999) 56-68.
[25] C.R. Shaddix, T.C. Williams, *American Scientist* 95 (2007) 232-239.
[26] T.C. Williams, C.R. Shaddix, K.A. Jensen, J.M. Suo-Anttila, *Int. J. Heat Mass Trans.* 50 (2007) 1616-1630.
[27] W.H Dalzell, A.F. Sarofim, *J. Heat Trans.* 91 (1969) 100-104.
[28] C.R. Shaddix, K.C. Smyth, *Combust. Flame* 107 (1996) 418-452.
[29] F. Liu, K.A. Thomson, G.J. Smallwood *Appl. Phys. B* 96 (2009) 671-682.
[30] T.C. Bond, R.H. Bergstrom, *Aerosol Sci. Tech.* 40 (2006) 27-67.
[31] B. Hu, B. Yang, U.O. Koylu, *Combust. Flame* 134 (2003) 93-106.
[32] B. Yang, U.O. Koylu, *Combust. Flame* 141 (2005) 55-65.
[33] A. Coppalle, D. Joyeux, *Combust. Flame* 96 (1994) 275-285.
[34] S.-Y. Lee, S.R. Turns, R.J. Santoro, *Combust. Flame* 156 (2009) 2264-2275.